

Received April 4, 2022, accepted April 13, 2022, date of publication April 18, 2022, date of current version April 26, 2022.

Digital Object Identifier 10.1109/ACCESS.2022.3168047

Application of the ISE Optimized Proportional Control of the Wave Maker in a Towing Tank

MARCIN DRZEWIECKI ^{id} AND JAROSLAW GUZINSKI, (Senior Member, IEEE)

Department of Electric Drives and Energy Conversion, Faculty of Electrical and Control Engineering, Gdańsk Tech, 80-233 Gdańsk, Poland

Corresponding author: Marcin Drzewiecki (marcin.drzewiecki@pg.edu.pl)

This work was supported by the Faculty of Electrical and Control Engineering, Gdańsk Tech.

ABSTRACT This paper presents the improvement of the wave maker control system. The wave maker is a facility widely used in hydromechanics laboratories to generate waves in towing tanks. It is equipped with an electrohydraulic drive and an actuator submerged into water. The waves are generated to model the environmental conditions for physical experiments, performed on reduced-scale models of maritime objects. The physical experiments allow to predict the behaviour of full-scale objects and prove the results of numerical analyses. The overriding goal of the fluid dynamics experiments is to improve the human safety and survivability of constructions. The reported investigation and application works were vital for the improvement of physical model tests. The optimization of the proportional controllers was performed in terms of the Integral of Squared Error (ISE). The final evaluation was performed in terms of the frequency response characteristic. The results of the proportional control optimization were evaluated versus the previously applied control. The experimental research was conducted in the real towing tank located at the Maritime Advanced Research Centre. The investigation has shown the advantage of the ISE optimized conventional proportional control. It has particularly proven the affordability and swiftness of the optimization process. It also proved a more efficient frequency response of the wave maker obtained within a required and reasonable lead time. The performed investigation has greatly contributed to the development of a new method of physical experiments in white noise waves. The results related to this new more efficient method are presented as well.

INDEX TERMS Automatic control, energy conversion, hydraulic actuators, ISE optimization, marine safety, microcontrollers, proportional control.

NOMENCLATURE

ω	Angular frequency.	H_c	Transfer function of the double acting hydraulic cylinder.
a	Amplitude of flap oscillations.	H_f	Transfer function of the flap submerged into water.
C_1	Inner controller of the stroke piston position.	H_h	Transfer function of the hydraulic pipes.
C_2	Outer controller of the hydraulic cylinder position.	H_p	Transfer function of the stroking mechanism.
e	Actuating signal.	H_s	Transfer function of the stroke piston.
E	Error function.	H_s	Significant height of the wave.
FFT	Fast Fourier Transform.	H_v	Transfer function of the servo valve.
h	Level of the waterplane above the bottom.	IAE	Integral of Absolute Error.
h_0	Level of the hinge above the bottom.	ISE	Integral of Squared Error.
H_1	Transfer function of the positioning module of the variable displacement electropump stroking mechanism.	ITAE	Integral of Time weighted Absolute Error.
H_2	Transfer function of the positioning module of the wave maker flap.	ITSE	Integral of Time weighted Squared Error.
		JONSWAP	Joint North Sea Wave Observation Project spectrum.
		k_{C_1}	Gain of the inner controller of stroke piston position.

The associate editor coordinating the review of this manuscript and approving it for publication was Xiaodong Liang ^{id}.

k_{C_2}	Gain of the outer controller of hydraulic cylinder position.
k_2	Gain of the positioning module of the wave maker flap.
k_f	Damper constant of the flap submerged into water.
k_h	Gain of the hydraulic pipes.
k_p	Gain of the pump displacement.
k_v	Gain of the servo valve.
M	Magnitude.
PCs	Proportional Controllers.
PID	Proportional-Integral-Derivative Controller.
R	Reference input signal.
RAO	Response Amplitude Operators.
RISC	Reduced Instruction Set Computer.
s	Imaginary argument of the Laplace transform.
T_{C_1}	Integration time of the inner controller of stroke piston position.
T_{C_2}	Integration time of the outer controller of hydraulic cylinder position.
T_0	Delay time of the hydraulic pipes.
T_1	Integration time of the positioning module of the variable displacement electropump stroking mechanism.
T_2	Integration time of the positioning module of the wave maker flap.
T_c	Integration time of the double acting hydraulic cylinder.
T_s	Integration time of the stroke piston.
TMA	Texel, Marsen, and Arsloe spectrum.
u	Control signal.
x_1	Stroke piston position signal.
x_2	Hydraulic cylinder position signal.
x_2^{ref}	Hydraulic cylinder position reference signal.

I. INTRODUCTION

Optimization of the water wave generation process in a towing tank is vital for physical modelling of environmental conditions in hydromechanics laboratories. The waves in towing tanks are mechanically generated using specialized research equipment - the wave makers. The optimized control system of the wave maker allows the wave profiles to be accurately modelled. Accurate modelling of wave profiles is required for proper experimental testing of the reduced-scale physical models [1], [2], conducted to enhance the safety and performance of maritime structures, such as ships, oil rigs, and wind turbines. Despite the well-developed computational fluid dynamics, the experimental fluid dynamics allows the results of numerical analysis to be physically proven [3]. According to the Buckingham theorem [4], physical experiments on the reduced-scale models (Fig. 1) allow to predict the properties of full-scale objects. This kind of research is widely carried out in hydromechanics laboratories [5]–



FIGURE 1. The reduced-scale free-running model of ship in the deepwater towing tank at the Maritime Advanced Research Centre [40].

[9]. Continuous improvement of experimental testing techniques has the background in the need for constant increase of maritime safety. Proper execution of the reduced-scale experiments is of great importance, as the human life and safety can be seriously affected by the full-scale maritime objects [10].

Past control approaches have mainly involved the wave makers generating the waves with the Pierson-Moskowitz, JONSWAP or TMA models of wave spectra [11]. The desired amplitudes of those kinds of spectra decrease for higher frequency bands [12]. Until now, the flap movement amplitude decreasing for higher frequency bands – as a consequence of a wave maker performance – was acceptable. Following the research on a new, alternative and more efficient method of predicting the motion of a full-scale object, the experiments in white noise waves were appointed as the new approach to experimental determination of the Response Amplitude Operators (RAO) [13], [14]. Due to the applied waves with profiles corresponding to the white noise spectrum, it was necessary to ensure a constant amplitude also for higher frequency bands. This motivated a further improvement of the frequency response with the use of affordable and swift optimization methods.

42.9% of the wave makers in towing tanks worldwide are reported as flap-type, 61.1% as a single unit, and 43.2% as equipped with a hydraulic driving mechanism [11]. The wave maker, considered in the reported experimental research is a commonly-used flap-type facility, presented in Fig. 2. It consists of the drive and the oscillating actuator, submerged into water. Proper control of the drive and, consequently, the actuator movements, allows to generate waves having the spectrum appropriate to model the target sea conditions in a reduced-scale. However, the newly appointed method of RAO evaluation with the use of white noise waves introduces a new model of wave spectrum [13], [14] which creates a challenge for further performance improvement of the existing wave makers. It requires securing a constant amplitude of the wave spectra along the frequency bands in a wider scope than it has been formerly developed for the great amount of the presently used wave makers.

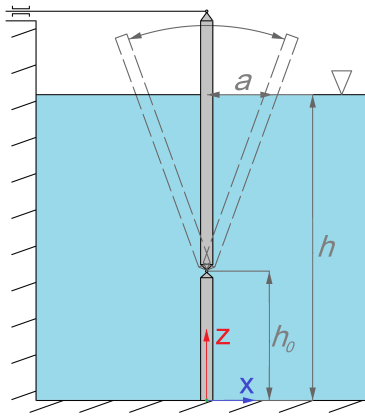


FIGURE 2. Side view of the wave maker: α —amplitude of flap oscillations, h —level of the waterplane above the bottom, h_0 —level of the hinge above the bottom [21].

The transfer function between the flap movement and the generated wave has already been presented in literature and follows from the linear wave maker theory [15]–[19]. It is specific to the geometry of the actuator and can be numerically derived [20], [21]. The experimental research has shown that the linear theory, named the 1st order theory, is applicable when generating waves of low steepness [22]–[25]. As a consequence of further research, the nonlinear wave maker theory, named the 2nd order theory, was derived [26] and further developed [27], [28]. The nonlinear wave maker theories covered numerous phenomena related to waves modeled both numerically [29]–[34] and experimentally [26], [35]–[38]. However, the issue regarding automatic and accurate generation of waves with the spectrum, reflecting the target sea conditions in a reduced-scale of physical experiment in a towing tank has only been finally solved with the use of the adaptive control approach [39]. In the first attempt, the control system consisted of proportional-integral controllers optimized in accordance with the Ziegler-Nichols parameters, wherein the ultimate gains and periods were collected using the Åström-Hägglund relay method [40], [41]. In the next attempt, the system consisted of the rule-based Mamdani-type fuzzy-logic control of flap position and velocity, according to the expertise of the authors [21]. The developed solution allowed to meet the required accuracy following from the procedures and guidelines regarding towing tanks [1], [2], [42]–[44], within the scope of the models of wave spectra applied and analysed at that time [12], [45].

The white noise model of spectra applied in the new method of RAO evaluation [13], [14] established the need to develop a new controller for the wave maker, which would have even more flat amplitude characteristic than those previously delivered [21]. This flat amplitude characteristic was expected to preserve constant amplitude of the white noise along a higher frequency bands. Simultaneously, following the queries raised in public discussion [39], in-depth identification of a more-persistently excited object – the wave

maker in a towing tank – was advisable. The fuzzy-logic controller was indicated as complex and not necessarily more effective in optimization and implementation than the classic PID-type controller. Further improvement of the frequency response was recommended to be searched for using optimization methods for PID-type controllers. The above identified research gaps needed to be filled, and this issue addressed in the paper.

The major contribution of the work presented in the paper includes:

- decrease of costs of physical experiments realization by facilitating a new alternative and more efficient method of experimental RAO determination with the use of white noise waves;
- wider availability of high-quality model tests for other towing tanks as a result of disclosure of a ready-made solution for modernization of existing research facilities to expand their working areas and to enable the implementation of newly appointed and more efficient physical experiments;
- significant improvement of maritime safety in terms of human security and survivability of constructions – as a result of physical experiments conducted with the use of white noise waves in towing tanks.

The paper is organized in the following way. Section I is a general introduction presenting the context and state of the art of the current study, and indicating its novelties and major contributions. The objectives and the scope of the research are discussed in Section II. The proposed and applied solution is presented in Section III. Section IV shows the model of the control system and the development of the solution. In particular, the model of the positioning module of the stroking mechanism of the variable-displacement electropump is introduced in subsection IV-A. The model of the positioning module of the wave maker flap is introduced in subsection IV-B. The ISE optimization is developed in subsection IV-C. Next, the obtained results and their positive validation are presented in Section V. The application and the validation of the developed solution are presented in subsections V-A and V-B, respectively. Section VI concludes the benefits of the performed study and indicates the future scope of research.

II. OBJECTIVES AND SCOPE

The new approach to the RAO method evaluation has been formulated and proven to be well efficient [13], [14]. This method needs to maintain consistent amplitude along the applied frequencies of the white noise spectrum. Within the research described in [39], a significant impact of the wave maker flap inertia and hydrodynamic loads on the flap movement was found. Consequently, the flap movement amplitude decreases when the desired wave frequency increases. The control methods used in the past [21], [39]–[41], [46] did not provide a flat frequency response of the wave maker, as a result of which the amplitudes of successive harmonic frequencies of the white noise were

reduced. The ISE optimization method was expected to improve the control system to ensure a constant amplitude along the applied frequencies and meet the required wave modeling accuracy [1], [2].

The objective of the present investigation was to develop an optimized conventional PID-type control and evaluate its operation versus the controllers hitherto successively applied: proportional-integral and fuzzy-logic. The evaluation was performed in terms of the desired flat frequency response characteristic. To meet these objectives, the in-depth identification of the wave maker and the optimization method of conventional controller tuning were involved. The experimental investigation was cost- and time-limited due to numerous commercial model tests intended to be performed in the towing tank. Therefore, any research work aiming to improve the properties of the wave maker was considerably limited in time. Hence, it was very important to investigate a simple control system with small number of parameters for tuning that would simultaneously provide the required quality of regulation. On the other hand, developing a model of the towing tank equipped with the wave maker for simulation research was inefficient due to the lack of a sufficiently general and robust hydromechanical model. Thus, the final tuning of the control system required to be carried out on a real object, the access to which was highly limited. The main contribution of the work was the improvement of performance of physical experiments, particularly those performed in white noise waves.

III. SOLUTION

To meet the objectives and scope discussed in the foregoing section, the wave maker elements were theoretically analysed and synthesized into two functional modules. Afterwards, they were experimentally identified while persistently excited by a white noise of relevant amplitudes and harmonics [47]. All signals were acquired using the *HBM Spider8 4.8 kHz* data acquisition module. The acquired signals were registered on a personal computer equipped with the *HBM Catman Professional 4.5* data acquisition software. The measurements were carried out with a sampling frequency of 25 Hz and 12-bit resolution in the range of ± 10 V. The numerical analysis and visualization of the results were performed with the use of *GNU Octave* [48]. All registered signals were analysed in frequency domain using the Fast Fourier Transform (FFT). The amplitudes of the harmonics were estimated with the use of the Welch's method [49].

The model of the control system was optimized with respect to the minimum value of ISE. The developed proportional controllers (PCs) were applied in a cascade arrangement in a 32-bit Advanced RISC Machine ARM microcontroller. The PCs were experimentally adjusted with respect to applicable gain values. The applied control system was launched and the frequency response was experimentally investigated in a white noise of persistently exciting amplitudes and harmonics [47]. Finally, the conventional proportional control was evaluated versus the fuzzy-logic control.

The PCs were validated and used in physical model tests in white noise waves. The subsequent steps and results of the research are detailed in the following sections.

IV. MODEL OF THE CONTROL SYSTEM

The considered wave maker is equipped with a hydraulic drive mechanism. The structure of the hydraulic circuits of the wave maker is detailed in Fig. 3. Following from the structure detailed there, two modules can be distinguished: the positioning module of the stroking mechanism of the variable displacement electropump, and the positioning module of the wave maker flap. The first – inner – module is the auxiliary oil circuit and consists of a stroke piston supplied by an auxiliary pump with servo valve. The second – outer – module is the main oil circuit and consists of a double-acting hydraulic cylinder supplied by a variable displacement electropump. These modules are detailed in the following subsections.

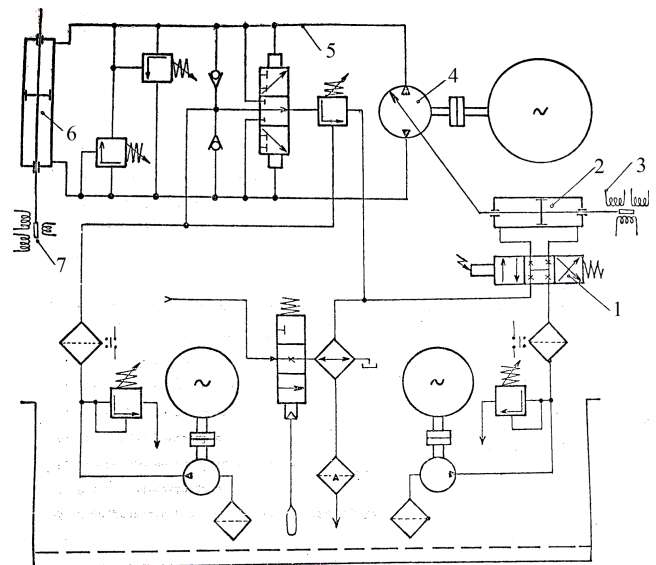


FIGURE 3. Structure of the hydraulic circuits of the wave maker: 1–proportional servo valve, 2–stroke piston, 3–stroke piston position sensor, 4–variable displacement electropump, 5–hydraulic circuits, 6–hydraulic cylinder, 7–hydraulic cylinder position sensor [51].

Fig. 4 shows the top view of the wave maker. Following from the construction shown there, the flap can be recognized to react with damping.

A. POSITIONING MODULE OF THE VARIABLE DISPLACEMENT ELECTROPUMP STROKING MECHANISM

The first of the analysed modules consists of an electrohydraulic servo valve and a stroke piston. The electrohydraulic servo valve is the *MOOG D634-501A* series *R40K02MONSM2* type. It is a proportional servo valve with integrated electronics and linear flow characteristic in relation to the voltage command signal [50]. Thus, the transfer function of the servo valve is

$$H_v(s) = k_v. \quad (1)$$

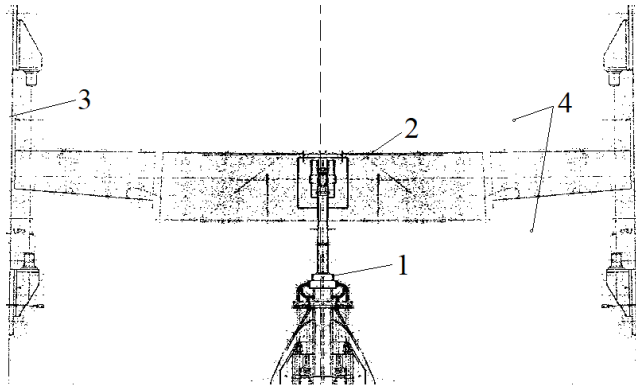


FIGURE 4. Top view of the wave maker: 1–hydraulic cylinder, 2–flap, 3–tank wall, 4–water surface [51].

The stroke piston is a hydraulic cylinder with hydraulic oil inlets and outlets to move the piston rod [51]. Thus, the transfer function of the stroke piston is

$$H_s(s) = \frac{1}{T_s s} \quad (2)$$

The derived terms were compounded in accordance with the structure of the positioning mechanism (Fig. 3). The compounding of the terms working in tandem, consists of the multiplication of (1) and (2). Thus, the transfer function of the positioning module of the stroking mechanism of the variable displacement electropump is

$$H_1(s) = \frac{1}{T_1 s}, \quad (3)$$

where T_1 is the resultant integration time of the module.

Along with analytical consideration of the structure, the module was identified experimentally. To achieve this, the stroke piston position signal x_1 was measured versus the control signal u whilst the white noise signal was given as the reference input x_2^{ref} (Fig. 9). The measured signals were registered and analysed.

The applied white noise signal was within the frequency band from 1.2 rad/s to 7.6 rad/s, with increment of 0.05 rad/s and had harmonic amplitudes of 0.125 V, 0.177 V and 0.217 V. The frequency band and the harmonic amplitudes were selected as relevant to persistent excitation of the actuators within their operating range [47]. The u and x_1 signals were acquired. The frequency response was calculated in frequency domain as the magnitude $M(\omega)$ of $x_1(\omega)$ related to $u(\omega)$ and expressed in decibels:

$$M(\omega) = 20 \log \left(\frac{x_1(\omega)}{u(\omega)} \right) \quad (4)$$

Consequently, the time $T_1 = 0.135$ s, was established to fit the model (3) to the results of the physical experiment. The frequency response of the established model is compared in Fig. 6 with that of the actual physical plant.

The consistency of the model (3) with the actual physical plant was evaluated as sufficient in term of frequency

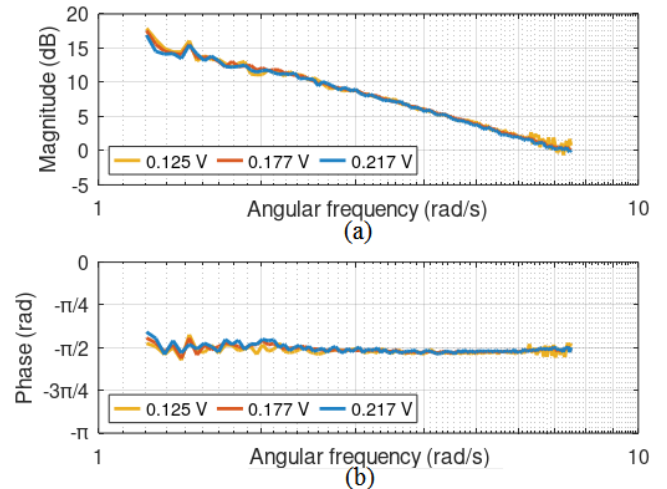


FIGURE 5. Frequency response of the positioning module of the stroking mechanism of the variable displacement electropump to white noise with an amplitudes of: 0.125 V, 0.177 V and 0.217 V. (a) Magnitude. (b) Phase.

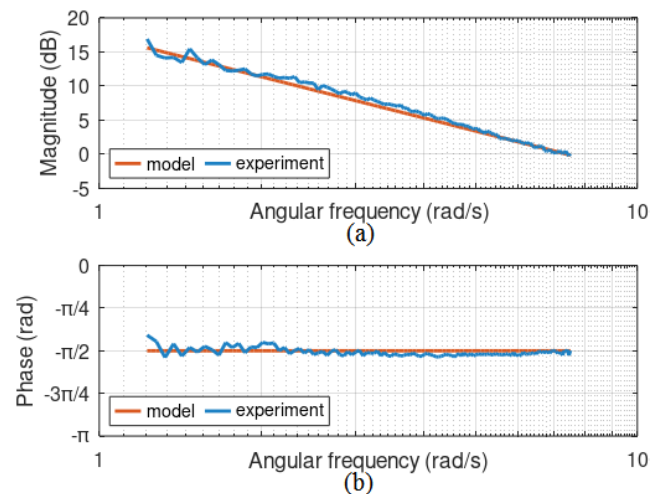


FIGURE 6. Frequency response of the positioning module of the stroking mechanism of the variable displacement electropump—model vs. experiment. (a) Magnitude. (b) Phase.

response. The developed model (3) was approved for application.

B. POSITIONING MODULE OF THE WAVE MAKER FLAP

The second of the analysed modules consists of a stroking mechanism of the variable displacement electropump, hydraulic pipes, a double acting hydraulic cylinder, and a flap submerged into water.

The variable displacement electropump is at constant speed [51]. Thus, the transfer function of its stroking mechanism is [52]:

$$H_p(s) = k_p, \quad (5)$$

where k_p is the pump displacement gain.

The hydraulic oil flows with some delay through the hydraulic pipes from inlet to outlet. Thus, the transfer

function of the hydraulic pipes is

$$H_h(s) = k_h e^{-sT_0(\omega)}, \tag{6}$$

where k_h is the hydraulic gain and $T_0(\omega)$ is the delay time that depends on the flap displacement frequency.

The double acting hydraulic cylinder is a body with hydraulic oil inlets and outlets that move the piston rod [51]. Thus, the transfer function of the double acting hydraulic cylinder is

$$H_c(s) = \frac{1}{T_c s}, \tag{7}$$

where T_c is the integration time of the double acting hydraulic cylinder.

The flap is submerged into water and is coupled with the piston rod of the double acting hydraulic cylinder. Following from Fig. 2 and Fig. 4, the flap submerged into water can be recognized as a damper that reacts to the displacement of the piston rod. Thus, the transfer function of the flap submerged into water is

$$H_f(s) = k_f s + 1, \tag{8}$$

where k_f is the damper constant.

The derived terms were compounded in accordance with the structure of the positioning mechanism (Fig. 3). The compounding of the terms working in tandem consists of the multiplication of (5)-(8). Thus, the transfer function of the positioning module of the wave maker flap is

$$H_2(s) = \frac{k_2 s + 1}{T_2 s} e^{-sT_0(\omega)}, \tag{9}$$

where k_2 and T_2 are the resultant constants and the resultant integration time of the module, respectively.

Along with analytical consideration of the structure, the module was identified experimentally. To achieve this, the hydraulic cylinder position signal x_2 was measured versus the signal x_1 , whilst the white noise signal was given as x_2^{ref} (Fig. 9). The measured signals were registered and analysed.

The applied white noise signal was within the frequency band from 1.2 rad/s to 7.6 rad/s, with increment of 0.05 rad/s, and had harmonic amplitudes of 0.125 V, 0.177 V and 0.217 V. The frequency band and the harmonic amplitudes were selected as relevant to persistent excitation of the actuators within their operating range [47]. The signals x_1 and x_2 were acquired. The frequency response was calculated in frequency domain as the magnitude $M(\omega)$ of $x_2(\omega)$ related to $x_1(\omega)$ and expressed in decibels:

$$M(\omega) = 20 \log \left(\frac{x_2(\omega)}{x_1(\omega)} \right). \tag{10}$$

Consequently, the values of $k_2 = 0.149$, $T_2 = 0.452$ s and $T_0 = 0.17$ s, were established to fit the model (9) to the results of the physical experiment. The frequency response of the established model (9) is compared in Fig. 8 with that of the actual physical plant.

The consistency of the model (9) with the actual physical plant was evaluated as sufficient in term of frequency

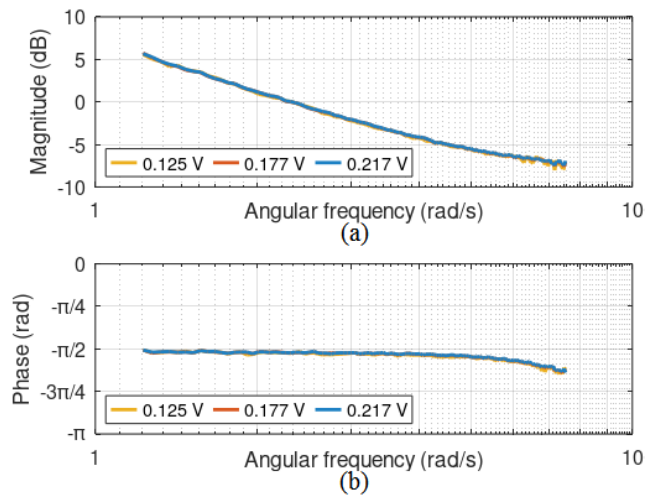


FIGURE 7. Frequency response of the positioning module of the wave maker flap to white noise with amplitudes of: 0.125 V, 0.177 V, and 0.217 V. (a) Magnitude. (b) Phase.

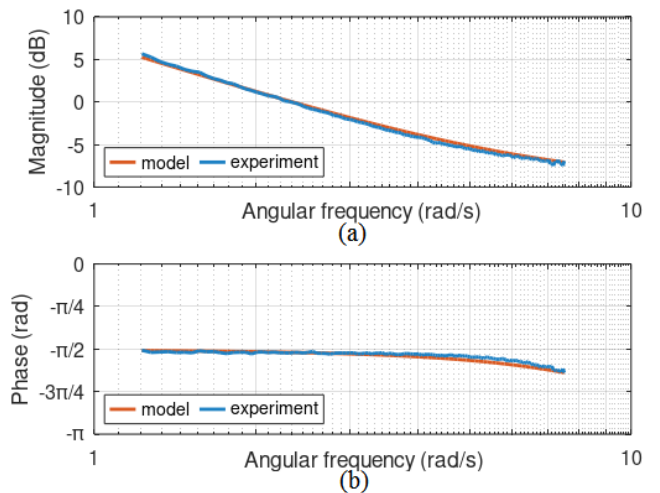


FIGURE 8. Frequency response of the positioning module of the wave maker flap—model vs. experiment. (a) Magnitude. (b) Phase.

response. The developed model (9) was approved for application.

C. ISE OPTIMIZATION

The control system consisting of the analysed modules needed to be optimized. The ISE is one of the most common minimum error criterium methods of tuning PID-type controllers [53], [54]. It minimizes the square value of the error at transient response, integrated in time. Along with the ISE optimization, the control system performance index was applied as

$$ISE = \int_0^{\infty} [e(t)]^2 dt, \tag{11}$$

wherein the ISE value is considered as the cost function.

This optimization method searches for optimal parameters of the controller to minimize the cost function (11) [54], [55].

The following cost functions based on integral of error have been considered: integral of the squared error (ISE), integral of the absolute error (IAE), integral of the time weighted square error (ITSE) and integral of the time weighted absolute error (ITAE). The IAE, ITSE and ITAE cost functions were recognized as difficult – versus the ISE – to deal with analytically and therefore omitted as long as the ISE method turns out satisfactory. This was done due to the fact that the control algorithms and settings of their terms were appointed as needed to be analytically pre-selected. The ISE optimization method was involved to improve the performance of conventional control of the control system shown in Fig. 9. The ISE method was chosen due to its efficiency and simplicity, resulting in fast implementation. This requirement was vital regarding the physical white noise experiment appointed for realization with the wave maker.

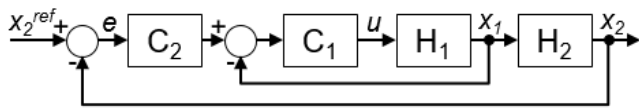


FIGURE 9. The structure of the cascade control system: C_1 inner controller of the stroke piston position and C_2 outer controller of the hydraulic cylinder position (H_1 -positioning module of the variable displacement electropump stroking mechanism, H_2 -positioning module of the wave maker flap, x_2^{ref} -reference input signal, e -actuating signal, u -control signal, x_1 -stroke piston position signal, x_2 -hydraulic cylinder position signal).

In the first attempt, the system was considered with the cascaded proportional-integral controllers of stroke piston and hydraulic cylinder positions – (12) and (13), respectively. For safety reasons, the derivative term was rejected in the related works [39] due to impermissible flap oscillations.

$$C_1(s) = k_{C1} \left(1 + \frac{1}{T_{C1}s} \right) \quad (12)$$

$$C_2(s) = k_{C2} \left(1 + \frac{1}{T_{C2}s} \right) \quad (13)$$

In accordance with the structure of the considered system (Fig. 9), the error function of the inner loop with the reference input $R(s)$, takes the form

$$E(s) = R(s) \cdot \frac{1}{1 + C_1(s)H_1(s)}. \quad (14)$$

After applying the reference input signal in the form of a unit step

$$R(s) = \frac{1}{s}, \quad (15)$$

together with (3) and (12) to (14), the error function takes the following general form

$$E(s) = \frac{c_0 + c_1s + \dots + c_ms^m}{d_0 + d_1s + \dots + d_ns^n}, \quad (16)$$

with $m = 1$ and $n = 2$, where: $c_0(s) = 0$, $c_1(s) = T_1 T_{C1}$, $d_0(s) = k_{C1}$, $d_1(s) = k_{C1} T_{C1}$, $d_2(s) = T_1 T_{C1}$.

Using the Krasovschi-Pospelov formulas [56], for the error function (16) with $m < n$, the ISE may be expressed as

$$ISE = \frac{c_1^2 d_0 + c_0^2 d_2}{2d_0 d_1 d_2} = \frac{T_1}{2k_{C1}}. \quad (17)$$

It can be derived from (17) that the value of ISE tends to zero, as k_{C1} tends to infinity. Meanwhile, it can be seen in (17) that T_{C1} does not affect the ISE value. This means that the inner loop is optimal – in the ISE (17) [56] sense – for large enough values of k_{C1} . The integral term of the inner controller is not involved in minimizing the ISE. Thus, the system was considered with the proportional controller of stroke piston position

$$C_1(s) = k_{C1}. \quad (18)$$

Consequently, the error function of the outer loop of the considered system (Fig. 9) with the reference input $R(s)$, takes the form

$$E(s) = R(s) \cdot \frac{1}{1 + C_2(s)C_1(s)H_1(s)H_2(s)}. \quad (19)$$

After applying the reference input signal in the form of (15) together with (3), (9), (13) and (18) to (19), the error function can be expressed in the general form (16), where $m = 2$ and $n = 3$. According to the general form: $c_0(s) = 0$, $c_1(s) = 0$, $c_2(s) = T_1 T_2 T_{C2}$, $d_0(s) = k_{C1} k_{C2}$, $d_1(s) = k_{C1} k_{C2} (T_{C2} k_2)$, $d_2(s) = k_2 k_{C1} k_{C2} T_{C2}$, $d_3(s) = T_1 T_2 T_{C2}$.

The positioning module of the wave maker flap was applied as

$$H_2(s) = \frac{k_2s + 1}{T_2s}. \quad (20)$$

The exponential term (9) representing delay is omitted in (20) to make the analytical ISE optimization feasible. The influence of delay will be analysed in further considerations.

Using the Krasovschi-Pospelov formulas [56] for the error function (16) with $m < n$, the ISE may be expressed as

$$\begin{aligned} rCIISE &= \frac{c_2^2 d_0 d_1 + (c_1^2 - 2c_0 c_2) d_0 d_3 + c_0^2 d_2 d_3}{2d_0 d_2 (d_1 d_2 - d_0 d_3)} \\ &= \frac{T_1 T_2 (T_{C2} + k_2)}{2k_2 k_{C1} k_{C2} (T_{C2} + k_2) - 2T_1 T_2}. \end{aligned} \quad (21)$$

It can be derived from (21) that the value of ISE tends to zero as k_{C1} and k_{C2} tend to infinity, also regardless of T_{C2} . This means that the considered system (Fig. 9) is optimal – in the ISE (21) [56] sense – for large enough values of k_{C1} and k_{C2} . The proportional terms of the cascaded controllers seem to be sufficient for minimizing the ISE (21). Thus, the system was finally approved for application with the PCs of stroke piston position (18) and hydraulic cylinder position (22).

$$C_2(s) = k_{C2} \quad (22)$$

The PCs – (18) and (22) – were intended for application with the maximum applicable gain values – k_{C1} and k_{C2} .

V. RESULTS AND VALIDATION

A. APPLICATION OF CONVENTIONAL PROPORTIONAL CONTROL

The conventional proportional controllers developed in the previous section were applied in a cascade arrangement (Fig. 9). In this structure, the analogue signals x_1 and x_2 are acquired with linear displacement transducers [46]. The acquired signals are processed in the recursive algorithms of the controllers arranged in a cascade to produce the u control signal, further processed with the wave maker actuators [46]. The digital-to-analogue conversion (DAC) is realized with the 12-bit resistor ladder of R-2R structure [57]. The analogue-to-digital conversion (ADC) is realized with the 12-bit successive approximation register (SAR) [58]. Besides, the signals are conditioned using external matching circuits [46]. The discrete-time control algorithm is applied in an interrupt-driven manner. The interrupt service routine is performed every 62 ms. The C# source code was developed in Microsoft Visual Studio [59] and .NET micro framework platform. The Microsoft.SPOT.Hardware namespace together with the STM32F429I_Discovery.Netmf.Hardware.cs managed library, were used [60]. The source code was deployed into the STM32F4 microcontroller with 32-bit ARM Cortex-M4 processor core. The embedded system, equipped with the STM32F4 microcontroller and Graphical User Interface, is presented in Figure 10.



FIGURE 10. The wave maker embedded system, equipped with the STM32F4 microcontroller and graphical user interface [40].

The PCs were initially applied with significant values of gains to minimize the ISE. This was due to the developed model. On the other hand, the limitation of gain values is indispensable to avoid sustained oscillations that occur above the ultimate gains of the actual physical system [61]. Several sets of gain values were applied successively. A qualitative

assessment was carried out to recognize the occurrence of impermissible oscillations. The results are collated in Table 1.

TABLE 1. Qualitative assessment of the occurrence of impermissible oscillations in steady state for selected gains $-k_{C1}$ and k_{C2} of inner and outer loop.

Application no.	1	2	3	4	5
k_{C1}	20	10	5	2.5	1.25
k_{C2}	10	5	2.5	1.25	1.25
Occurrence of oscillations	YES	YES	YES	YES	NO

The above process resulted in experimental selection of the applicable gains values, intended to minimize the ISE value without the occurrence of oscillations. The gain values were selected as $k_{C1} = 1.25$ and $k_{C2} = 1.25$. The control system was successfully run and could be assessed in the validation process.

B. VALIDATION OF CONVENTIONAL PROPORTIONAL CONTROL

The validation of the control algorithm applied in the previous subsection aimed to evaluate the applied control system in term of frequency response. The control system is expected to provide consistent harmonic amplitudes of flap position. It has to avoid decreasing the harmonic amplitudes for subsequent harmonic frequencies within the operating range of the wave maker [39], [51]. Thus, the frequency response – understood as the frequency-amplitude characteristic – is desired to be flat.

The validation was performed within the actual physical system – the flap-type wave maker, immersed in the deep-water towing tank [51]. The validation scenario included experimental evaluation of the frequency response of the object. The evaluation was performed within the newly applied conventional proportional control versus the controllers previously applied: proportional-integral [40], and fuzzy-logic [21]. It was assumed that the properly tuned proportional controllers may provide a more flat frequency response characteristic and then would be evaluated as superior over the hitherto applied solutions. To evaluate this, the signal x_2 was measured whilst the white noise reference signal was given as x_2^{ref} . The evaluation was done for proportional and fuzzy-logic control algorithms. The measured signals were registered and analysed.

The applied white noise signal was within the frequency band from 1.2 rad/s to 7.6 rad/s with increment of 0.05 rad/s, and had the harmonic amplitude of 0.125 V. The frequency band and the harmonic amplitude were selected to cover the operating range of the wave maker. The signal x_2 was acquired with the linear displacement transducer. The frequency response was calculated in frequency domain as the magnitude $M(\omega)$ of $x_2(\omega)$ related to $x_2^{ref}(\omega)$ and expressed in decibels:

$$M(\omega) = 20 \log \left(\frac{x_2(\omega)}{x_2^{ref}(\omega)} \right). \tag{23}$$

The proportional-integral control algorithm was investigated in the scope of the related work [40]. The sinusoidal input signals having frequencies from 1.3 rad/s to 7.6 rad/s, with increment of 0.63 rad/s, and amplitudes of 1 V were applied there. The frequency response was also calculated in decibels.

In accordance with the results of the numerical analysis, visualized in Fig. 11 and Fig. 12:

- the proportional-integral control algorithm provides the frequency response with the scope of 15.21 dB, in the range from -13.5 dB to 1.71 dB;
- the fuzzy-logic control algorithm provides the frequency response with the scope of 6.07 dB, in the range from -7.49 dB to -1.42 dB;
- the proportional control algorithm provides the frequency response with the scope of 4.28 dB, in the range from -5.51 dB to -1.23 dB.

All this proves that the proportional algorithm ensures more flat frequency response. Hence, the newly applied proportional control algorithm has been experimentally proven as more efficient over the previously applied solutions.

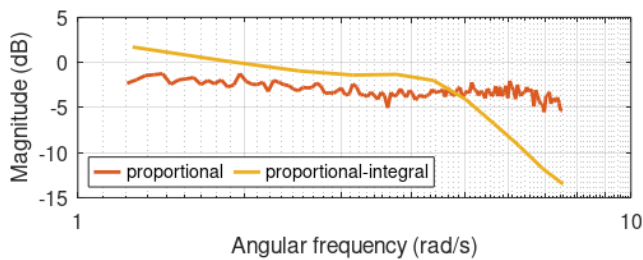


FIGURE 11. Frequency response of the wave maker with the controllers applied—proportional vs. proportional-integral [40].

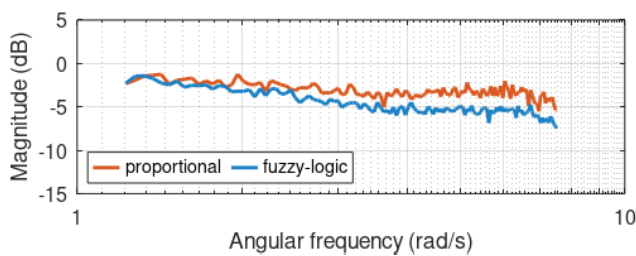


FIGURE 12. Frequency response of the wave maker with the controllers applied—proportional vs. fuzzy-logic.

The amplitude characteristics presented in Fig. 11 and Fig. 12 result from the viscous damping and the added mass impact on the flap movement. This is the consequence of the fact that the wave maker flap is immersed in water. As the frequency increases, the flap movements are more constrained by the viscous damping and the added mass. The added mass reflects the inertia arising from hydrodynamic loads. It has been discussed in detail in [39].

On the basis of the frequency responses determined experimentally, it was already recognized that the previously

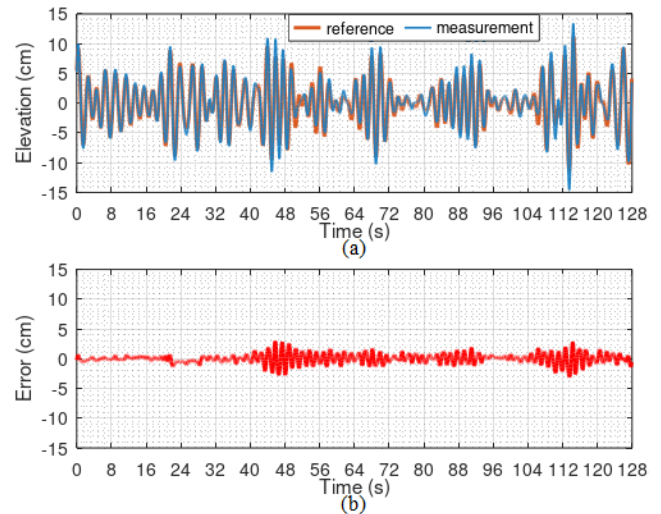


FIGURE 13. Free-surface water elevation in the towing tank while modeling of environmental conditions at the white noise wave with proportional control—measurement vs reference. (a) The white noise wave. (b) Error.

applied solutions did not meet the expectations to the same extent as the one developed by the authors within the works described in the paper. The aim of the presented work was to implement the most optimal method under the criterion of the expected flat amplitude characteristic. Consequently, the physical experiment appointed for realization in white noise waves was realized with the use of PCs. The white noise waves were physically modelled, measured, and analysed. The reference white noise wave was required with the harmonic amplitude of 0.91 cm. The corresponding significant height of the reference white noise wave $H_s^{reference}$ was equal to 14.83 cm. The wave profiles were measured using the invented method and an ultra-sound device [62]. The ultra-sound device probe position was in the axis of the towing tank at a distance of 105 m corresponding to half the length of the measurement section. The results of the measurements are presented in Fig. 13 and Fig. 14. The waveforms presented in Fig. 13 show that the modelling error increases noticeably after 43 seconds, due to the motion of reflected waves propagating away from the other end of the towing tank. The presence of the reflected waves is a consequence of limited absorption of the generated waves. This type of waves and the issues related to their absorption were out of scope of the present study. The frequency response was calculated in the frequency domain as the magnitudes related to the reference white noise waves and expressed in decibels, as presented in Fig. 13. The significant height of the measured white noise wave $H_s^{measurement}$ was equal to 15.45 cm. The white noise waves were modelled with an accuracy of 4%.

In accordance with the results presented in Fig. 14, the proportional algorithm provides the generation of white noise waves with the required $\pm 5\%$ accuracy of modelling the significant height H_s [1], [2]. It has been achieved in one adaptation loop [39] without the need for application the

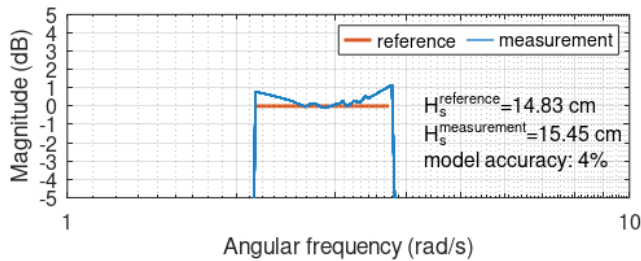


FIGURE 14. Frequency response characteristics of wave modelling of environmental conditions at the white noise wave with proportional control—measurement vs. reference.

iterative corrections performed one after the other. Hence, the proportional control algorithm has been proven to be greatly efficient as a new method of physical experiments in white noise waves.

VI. CONCLUSION

The results of the research described in the paper meet the objectives. The conventional proportional control was successively developed using the ISE optimization and applied. It provided an accuracy of 4% in modelling of H_s , therefore the desired accuracy of modelling the environmental conditions in the scope of the wave profile has been met. The proportional control ensures a more flat frequency response of the control system: it provides the frequency response within the scope of 4.28 dB, versus the scope of 15.21 dB for the proportional-integral control and of 6.07 dB for the fuzzy-logic control. This means that the proportional algorithm more efficiently overcomes the delays in the actual physical object. Thus the newly applied PCs were experimentally proven as superior over the previously applied controllers. This is in particular due to the complexity of the fuzzy-logic controller design and optimization processes, and the required tools and time. The investigation has proven that a more efficient frequency response of the wave maker is obtained with the ISE optimized proportional control, within a reasonable lead time required for the realization of model tests.

The advantages of the applied PCs improve the modelling of environmental conditions on a reduced-scale. This is especially true with regard to physical experiments in white noise waves, appointed for realization as a more efficient method. Properly optimized proportional control improves the efficiency of prediction of properties of a full-scale object and enables efficient experimental verification of the numerical analysis.

The presented solution is a ready-made for flap-type single unit wave makers equipped with a hydraulic driving mechanism. It can be easily and broadly applied to modernize and adapt the existing research facilities for the realization of a new, more efficient technique of experimental RAO determination.

Ultimately, the results of the work presented in the paper, significantly contribute to maritime safety.

As the future scope of the research, it is desirable to consider and implement active absorption of the reflected waves with the use of the developed control algorithm. It is considered to direct further research towards active absorption of reflected waves. This would allow for decrease of the modelling error and further improvement in the accuracy of modelling of environmental conditions. As the future scope of the research, it is also purposeful to optimize the control system in terms of the phase characteristic. This would allow for better reproduction of deterministic waves. Furthermore, if the ISE method was found to be insufficient for the future scope issues, other methods such as IAE, ITSE, and ITAE should be reconsidered.

REFERENCES

- [1] A. Iafrazi, D. Drazen, C. Kent, T. Fujiwara, Z. Zong, Y. Ma, H. J. Kim, L. Xiao, J. Hennig, and J. Sharnke, "Laboratory modelling of waves: Regular, irregular and extreme events," *ITTC Qual. Syst. Manual Recommended Procedures Guidelines*, vol. 2017, p. 8, Sep. 2017. [Online]. Available: <https://www.ittc.info/media/8095/75-02-07-012.pdf>
- [2] A. Iafrazi, T. Fujiwara, H. J. Kim, Y. Ma, J. Sharnke, S. C. Yim, P. C. Mello, X. Zhang, and M. Drzewiecki, "Recommended procedures and guidelines, guideline, laboratory modelling of waves," *ITTC Qual. Syst. Manual*, p. 14, Jun. 2021. [Online]. Available: <https://www.ittc.info/media/9697/75-02-07-012.pdf>
- [3] H. Khan, A. Ahsan, and K. A. Chaudhry, "Review of modern trend for numerical model testing in worldwide towing tanks," in *Proc. 16th Int. Bhurban Conf. Appl. Sci. Technol. (IBCAST)*, Jan. 2019, pp. 732–743. [Online]. Available: <https://ieeexplore.ieee.org/document/8667239/>, doi: 10.1109/IBCAST.2019.8667239.
- [4] E. Buckingham, "On physically similar systems; illustrations of the use of dimensional equations," *Phys. Rev.*, vol. 4, no. 4, pp. 345–376, Oct. 1914, doi: 10.1103/PhysRev.4.345.
- [5] A. C. Dubey, V. A. Subramanian, V. J. Kumar, and B. Bhikkaji, "Development of autonomous system for scaled ship model for seakeeping tests," in *Proc. OCEANS MTS/IEEE Monterey*, Sep. 2016, pp. 1–5. [Online]. Available: <https://ieeexplore.ieee.org/document/7761455/>, doi: 10.1109/OCEANS.2016.7761455.
- [6] X. Guo and B. Yu, "The forecast of ship speedability based on model test," in *Proc. 2nd Int. Conf. Mechanic Autom. Control Eng.*, Jul. 2011, pp. 3655–3658. [Online]. Available: <https://ieeexplore.ieee.org/document/5987786/>, doi: 10.1109/MACE.2011.5987786.
- [7] M. Ueno, T. Nimura, T. Fujiwara, and K. Nonaka, "Evaluation of RTK-OTF positioning system for free running manoeuvrability test of a model ship," in *Proc. MTS/IEEE Conf. (OCEANS)*, vol. 2, Oct. 1997, pp. 1120–1125. [Online]. Available: <https://ieeexplore.ieee.org/document/624149/>, doi: 10.1109/OCEANS.1997.624149.
- [8] L. Luznik, K. A. Flack, E. E. Lust, and D. P. Baxter, "Hydrodynamic performance of a horizontal axis tidal turbine under steady flow conditions," in *Proc. Oceans*, 2012, pp. 1–4. [Online]. Available: <https://ieeexplore.ieee.org/document/6404873/>, doi: 10.1109/OCEANS.2012.6404873.
- [9] M. W. Kindel and M. R. Dhanak, "Seakeeping response of a surface effect ship in near-shore transforming seas," in *Proc. Oceans*, Oct. 2012, pp. 1–6. [Online]. Available: <https://ieeexplore.ieee.org/document/6405096/>, doi: 10.1109/OCEANS.2012.6405096.
- [10] L. Zhu, L. Zhang, X. Li, and R. Zhou, "Maritime safety assessment in the 21st-century maritime silk road under risk factors coupling," in *Proc. 5th Int. Conf. Transp. Inf. Saf. (ICTIS)*, Jul. 2019, pp. 411–415. [Online]. Available: <https://ieeexplore.ieee.org/document/8883809/>, doi: 10.1109/ICTIS.2019.8883809.
- [11] A. Iafrazi, D. Drazen, C. Kent, T. Fujiwara, Z. Zong, Y. Ma, H. J. Kim, L. Xiao, J. Hennig, and J. Sharnke, "Report of the specialist committee on modelling of environmental conditions," in *Proc. 28th ITTC*, vol. 2, 2017, pp. 757–778. [Online]. Available: <https://www.ittc.info/media/7829/21-sc-modelling-environmental-conditions.pdf>
- [12] C. T. Stansberg, G. Contento, S. W. Hong, M. Irani, S. Ishida, R. Mercier, Y. Wang, J. Wolfram, J. Chaplin, and D. Kriebel, "Final report and recommendations to the 23rd ITTC," in *Proc. 23rd ITTC*, vol. 2, 2002, pp. 544–551. [Online]. Available: <https://itc.info/media/1469/waves.pdf>

- [13] S. Bielicki, A. Bednarek, and M. Kraskowski, "Evaluation of response amplitude operator of ship roll motions based on the experiments in white noise waves," in *Proc. 7B, Ocean Eng.*, Jun. 2017, Art. no. V07BT06A022, doi: [10.1115/OMAE2017-62555](https://doi.org/10.1115/OMAE2017-62555).
- [14] S. Bielicki, "Prediction of ship motions in irregular waves based on response amplitude operators evaluated experimentally in noise waves," *PMR*, vol. 28, no. 109, pp. 16–27, 2021, doi: [10.2478/pomr-2021-0002](https://doi.org/10.2478/pomr-2021-0002).
- [15] T. H. Havelock, "Forced surface-wave on water," *Phil. Mag.*, vol. 8, no. 51, pp. 569–576, 1929.
- [16] F. Biésel and F. Suquet, "Les appareils en générateurs laboratoire," *La Houille Blanche*, vol. 2, pp. 147–165, Mar. 1951.
- [17] F. Biésel and F. Suquet, "Les appareils en générateurs laboratoire," *La Houille Blanche*, vol. 4, pp. 475–496, Jun. 1951.
- [18] F. Biésel and F. Suquet, "Les appareils en générateurs laboratoire," *La Houille Blanche*, vol. 5, pp. 723–737, May 1951.
- [19] F. Biésel and F. Suquet, "Les appareils en générateurs laboratoire," *La Houille Blanche*, vol. 6, pp. 779–801, Dec. 1952.
- [20] M. Drzewiecki and W. Sulisz, "Generation and propagation of nonlinear waves in a towing tank," *Polish Maritime Res.*, vol. 26, no. 1, pp. 125–133, Mar. 2019, doi: [10.2478/pomr-2019-0014](https://doi.org/10.2478/pomr-2019-0014).
- [21] M. Drzewiecki and J. Guziński, "Fuzzy control of waves generation in a towing tank," *Energies*, vol. 13, no. 8, p. 2049, Apr. 2020, doi: [10.3390/en13082049](https://doi.org/10.3390/en13082049).
- [22] F. Ursell, R. G. Dean, and Y. S. Yu, "Forced small-amplitude water waves: A comparison of theory and experiment," *J. Fluid Mech.*, vol. 7, no. 1, pp. 33–52, Jan. 1960.
- [23] C. J. Galvin, *Wave-Height Prediction for Wave Generators in Shallow Water*, no. 4. Washington, DC, USA: U.S. Army Corps of Engineers, 1964, pp. 1–20.
- [24] T. Keating and N. B. Webber, "The generation of periodic waves in a laboratory channel; a comparison between theory and experiment," in *Proc. Inst. Civil Eng.*, vol. 63, 1977, pp. 819–832.
- [25] C. Campos, F. Silveira, and M. Mendes, "Waves induced by non-permanent paddle movements," in *Proc. Coastal Eng.*, vol. 13, 1972, pp. 707–722.
- [26] W. Sulisz and R. T. Hudspeth, "Complete second-order solution for water waves generated in wave flumes," *J. Fluids Struct.*, vol. 7, no. 3, pp. 253–268, Apr. 1993.
- [27] J. Spinneken and C. Swan, "Second-order wave maker theory using force-feedback control. Part I: A new theory for regular wave generation," *Ocean Eng.*, vol. 36, no. 8, pp. 539–548, Jun. 2009.
- [28] J. Spinneken and C. Swan, "Second-order wave maker theory using force-feedback control. Part II: An experimental verification of regular wave generation," *Ocean Eng.*, vol. 36, no. 8, pp. 549–555, Jun. 2009.
- [29] R. H. Multer, "Exact nonlinear model of wave generation," *J. Hydraulic Res.*, vol. 99, pp. 31–46, Jan. 1973.
- [30] S. T. Grilli and J. Horrillo, "Numerical generation and absorption of fully nonlinear periodic waves," *J. Eng. Mech.*, vol. 123, no. 10, pp. 1060–1069, Oct. 1997.
- [31] S.-X. Liu, B. Teng, and Y.-X. Yu, "Wave generation in a computation domain," *Appl. Math. Model.*, vol. 29, no. 1, pp. 1–17, Jan. 2005.
- [32] X. T. Zhang, B. C. Khoo, and J. Lou, "Wave propagation in a fully nonlinear numerical wave tank: A desingularized method," *Ocean Eng.*, vol. 33, nos. 17–18, pp. 2310–2331, Dec. 2006.
- [33] J.-H. Zheng, M. M. Soe, C. Zhang, and T.-W. Hsu, "Numerical wave flume with improved smoothed particle hydrodynamics," *J. Hydrodynamics*, vol. 22, no. 6, pp. 773–781, Dec. 2010.
- [34] X. Liu, P. Lin, and S. Shao, "ISPH wave simulation by using an internal wave maker," *Coastal Eng.*, vol. 95, pp. 160–170, Jan. 2015.
- [35] O. S. Madsen, "On the generation of long waves," *J. Geophys. Res.*, vol. 76, no. 36, pp. 8672–8683, Dec. 1971.
- [36] R. T. Hudspeth and W. Sulisz, "Stokes drift in 2-D wave flumes," *J. Fluid Mech.*, vol. 230, pp. 209–229, Sep. 1991.
- [37] W. I. Moubayed and A. N. Williams, "Second-order bichromatic waves produced by generic planar wavemaker in a two-dimensional wave flume," *J. Fluids Struct.*, vol. 8, no. 1, pp. 73–92, Jan. 1994.
- [38] H. A. Schaffer, "Second-order wavemaker theory for irregular waves," *Ocean Eng.*, vol. 23, pp. 47–88, Jan. 1996.
- [39] M. Drzewiecki, "An adaptive control of the wave in a towing tank," Ph.D. dissertation, Dept. Elect. Control Eng., Gdansk Tech, Gdansk, Poland, 2020.
- [40] M. Drzewiecki, "Control of the waves in a towing tank with the use of a black-box model," *ZN WEiA PG*, vol. 59, pp. 37–42, Sep. 2018, doi: [10.32016/1.59.07](https://doi.org/10.32016/1.59.07).
- [41] M. Drzewiecki, *Modelling, Simulation and Optimization of the Wave-maker in a Towing Tank*, vol. 577. Cham, Switzerland: Springer, 2017, pp. 570–579, doi: [10.1007/978-3-319-60699-6_55](https://doi.org/10.1007/978-3-319-60699-6_55).
- [42] P. Gualeni, J. F. Leguen, S. Cho, A. Cura-Hochbaum, T. Katayama, S. Ma, A. Matsuda, and A. M. Reed, "Recommended procedures and guidelines, procedure, model tests on damage stability in waves," *ITTC Qual. Syst. Manual*, vol. 2017, p. 8, Sep. 2017. [Online]. Available: <https://www.ittc.info/media/8145/75-02-07-042.pdf>
- [43] P. Jong, C. Kent, B. Bouscasse, F. Gerhardt, O. A. Hermundstad, T. Katayama, M. Minoura, B.-W. Nam, and Y. L. Young, "Recommended procedures and guidelines, procedure, seakeeping experiments," *ITTC Qual. Syst. Manual*, vol. 2021, pp. 1–13, Jun. 2021. [Online]. Available: <https://www.ittc.info/media/9705/75-02-07-021.pdf>
- [44] P. Jong, C. Kent, B. Bouscasse, F. Gerhardt, O. A. Hermundstad, T. Katayama, M. Minoura, B.-W. Nam, and Y. L. Young, "Recommended procedures and guidelines, procedure, HSMV seakeeping tests," *ITTC Qual. Syst. Manual*, vol. 2021, pp. 1–14, Jun. 2021. [Online]. Available: <https://www.ittc.info/media/9675/75-02-05-04.pdf>
- [45] C. A. R. Castillo, L. Xiao, V. Magarovskii, R. H. Yuck, H. Lie, Q. Xiao, A. Mentes, and Y. Nihei, "Recommended procedures and guidelines, procedure, analysis procedure of model tests in irregular waves," *ITTC Qual. Syst. Manual*, vol. 2021, pp. 1–6, Jun. 2021. [Online]. Available: <https://www.ittc.info/media/9729/75-02-07-0314.pdf>
- [46] M. Drzewiecki, "Digital control system of the wavemaker in the towing tank," *Automatyka, Elektryka, Zakłócenia*, vol. 7, no. 4, pp. 138–146, Dec. 2016, doi: [10.17274/AEZ.2016.26.08](https://doi.org/10.17274/AEZ.2016.26.08).
- [47] L. Ljung, "Characterization of the concept of 'persistently exciting' in the frequency domain," Dept. Autom. Control, Lund Inst. Technol., Lund, Sweden, Res. Rep. TFRT-3038, 1971.
- [48] J. W. Eaton. (2017). *GNU Octave Ver. 4.2.1*. [Online]. Available: <https://www.gnu.org/software/octave/>
- [49] P. Welch, "The use of fast Fourier transform for the estimation of power spectra: A method based on time averaging over short, modified periodograms," *IEEE Trans. Audio Electroacoust.*, vol. AE-15, no. 2, pp. 70–73, Dec. 1967. [Online]. Available: <https://ieeexplore.ieee.org/document/1161901>, doi: [10.1109/TAU.1967.1161901](https://doi.org/10.1109/TAU.1967.1161901).
- [50] *Drive Proportional Valves Series D633 and D634*, Servo Valve Catalog, MOOG, Elma, NY, USA, 2009.
- [51] F. Lechevallier, "12 metre wave generator operator's manual," ALSTHOM Techn. Des Fluids, Maritime Adv. Res. Centre, Gdansk, Poland, Tech. Rep., Mar. 1974.
- [52] H.-X. Cui, K. Feng, H.-L. Li, and J.-H. Han, "Response characteristics analysis and optimization design of load sensing variable pump," *Math. Problems Eng.*, vol. 2016, pp. 1–10, Jan. 2016, doi: [10.1155/2016/6379121](https://doi.org/10.1155/2016/6379121).
- [53] K. M. Hussain, R. A. R. Zepherin, M. S. Kumar, and S. M. G. Kumar, "Comparison of PID controller tuning methods with genetic algorithm for FOPTD system," *Int. J. Eng. Res. Appl.*, vol. 4, no. 2, pp. 308–314, 2014. [Online]. Available: <https://core.ac.uk/download/pdf/27178122.pdf>
- [54] C. Calistru, "Intelligent PID robust control based on integral criteria," in *Proc. 11th WSEAS Int. Conf. Autom. Control, Modelling Simulation*, 2009, pp. 534–539.
- [55] V. Rajinikanth and K. Latha, "Tuning and retuning of PID controller for unstable systems using evolutionary algorithm," *Int. Scholarly Res. Notices*, vol. 2012, pp. 1–11, May 2012, doi: [10.5402/2012/693545](https://doi.org/10.5402/2012/693545).
- [56] C.-N. Calistru, "A symbolic optimization approach for tuning of PID controllers," in *Proc. Int. Conf. Control Appl.*, 1995, pp. 174–175, doi: [10.1109/CCA.1995.555663](https://doi.org/10.1109/CCA.1995.555663).
- [57] B. Razavi, "The R-2R and C-2C ladders [a circuit for all seasons]," *IEEE Solid State Circuits Mag.*, vol. 11, no. 3, pp. 10–15, Aug. 2019, doi: [10.1109/MSSC.2019.2922886](https://doi.org/10.1109/MSSC.2019.2922886).
- [58] M. M. Pilipko and M. E. Manokhin, "Design of a low-power 12-bit SAR ADC," in *Proc. IEEE Conf. Russian Young Researchers Electr. Electron. Eng. (EIConRus)*, Jan. 2019, pp. 129–131. [Online]. Available: <https://ieeexplore.ieee.org/document/8657039>, doi: [10.1109/EIConRus.2019.8657039](https://doi.org/10.1109/EIConRus.2019.8657039).
- [59] Microsoft Corporation. (2012). *Microsoft Visual Studio Express 2012 for Windows Desktop*. [Online]. Available: <https://visualstudio.microsoft.com/vs/older-downloads/>
- [60] J. Kühner, "Introducing the .NET micro framework," in *Expert.NET Micro Framework*. New York, NY, USA: Apress, 2009, pp. 1–14, doi: [10.1007/978-1-4302-2388-7_1](https://doi.org/10.1007/978-1-4302-2388-7_1).

- [61] K. Aström and T. Hägglund, “Ziegler-Nichols’ and related methods,” in *PID Controllers: Theory, Design, and Tuning*, 2nd ed. Research Triangle Park, NC, USA: ISA, 1995, p. 137.
- [62] M. Drzewiecki, “A method and an ultra-sound device for a wave profile measurement in real time on the surface of liquid, particularly in a model basin,” Eur. Patent Appl. EP 19 460 026.8, European Patent Office, Munich, Germany, May 2019.



MARCIN DRZEWIECKI received the B.Sc.Eng., M.Sc.Eng., and Ph.D.Eng. degrees from the Faculty of Electrical and Control Engineering, Gdańsk Tech, Gdańsk, Poland, in 2012, 2015, and 2020, respectively. He was a Specialist with the Research and Development Department, Maritime Advanced Research Centre (CTO S.A.). He obtained scholarships in two research projects co-financed from European funds, and was granted with three scientific projects supported by the Polish Government and CTO S.A. in the area of development and implementation of the control systems of the wave makers. Since 2019, he has been a Research and Teaching Assistant with Gdańsk Tech, where he is currently an Assistant Professor. His research interests include control of the wave makers and water energy conversion systems. He was a member of the Specialist Committee on Modeling of Environmental Conditions at the 29th Conference of the ITTC—non-governmental organization with observer status to the International Maritime Organization, where ITTC participates actively in matters regarding safety and performance.



JAROSLAW GUZINSKI (Senior Member, IEEE) received the M.Sc., Ph.D., and D.Sc. degrees from the Electrical Engineering Department, Gdańsk Tech, Gdańsk, Poland, in 1994, 2000, and 2011, respectively. From 2016 to 2019, he was an Associate Professor with Gdańsk Tech, where he has been a Full Professor, since 2020. He is currently the Associate Dean of Science, as well as the Head of the Department of Electric Drives and Energy Conversion. He obtained scholarships in the Socrates/Erasmus Program, and was granted with three scientific projects supported by the Polish Government in the area of sensorless control and diagnostic for drives with LC filters. He has authored and coauthored more than 150 journals and conference papers. He is an inventor of some solutions for speed sensorless drives with LC filters (six patents). His research interests include sensorless control of electrical machines, multiphase drives (five-phase), inverter output filters, renewable energy, and electrical vehicles. He was awarded by the Polish Academy of Sciences—Division IV: Engineering Sciences for his monograph “Electric drives with induction motors and inverters output filters—selected problems,” in 2012.

...